Journal of Neurochemistry, 2006, **99**, 20–28 doi:10.1111/j.1471-4159.2006.04003.x

The substrate specificity of a neuronal glutamate transporter is determined by the nature of the coupling ion

David Menaker, Annie Bendahan and Baruch I. Kanner

Department of Biochemistry, Hebrew University Hadassah Medical School, Jerusalem, Israel

Abstract

Glutamate transporters are essential for terminating synaptic transmission. Glutamate is translocated together with three sodium ions. In the neuronal glutamate transporter EAAC1, lithium can replace sodium. To address the question of whether the coupling ion interacts with the 'driven' substrate during co-transport, the kinetic parameters of transport of the three substrates, L-glutamate and D- and L-aspartate by EAAC-1 in sodium- and lithium-containing media were compared. The major effect of the substitution of sodium by lithium was on K_m. In the presence of sodium, the values for K_m and I_{max} of these substrates were similar. In the presence of lithium, the K_m for L-aspartate was increased around 13-fold. Remarkably, the corresponding increase for L-glutamate and D-aspartate was much larger, around 130-fold. In marked contrast, the K_i values for a non-transportable substrate analogue were similar in the presence of either sodium or lithium. The preference for L-aspartate in the presence of lithium was also observed when electrogenic transport of radioactive substrates was monitored in EAAC1-containing proteoliposomes. Our results indicate that, subsequent to substrate binding, the co-transported solutes interact functionally in the binding pocket of the transporter.

Keywords: coupling ions, neuronal glutamate transporter, radioactive uptake, reconstitution, substrate specificity, transport currents.

J. Neurochem. (2006) **99**, 20–28.

Glutamate is the major excitatory neurotransmitter in the central nervous system and is removed from the synapse, and its surroundings, by glutamate transporters. Glutamate uptake is an electrogenic process (Kanner and Sharon 1978; Brew and Attwell 1987) in which the transmitter is co-transported with three sodium ions and one proton (Zerangue and Kavanaugh 1996a; Levy *et al*. 1998) followed by the counter-transport of one potassium ion (Kanner and Bendahan 1982; Pines and Kanner 1990; Kavanaugh *et al*. 1997). The mechanism involving two half cycles is supported by the fact that mutants impaired in potassium interaction are locked in an obligatory exchange mode (Kavanaugh *et al*. 1997; Zhang *et al*. 1998). Glutamate transporters mediate two distinct types of substrate-induced current: (i) an inward-rectifying current, reflecting electrogenic sodium-coupled glutamate translocation and (ii) an 'uncoupled' current, carried by chloride ions which is also activated in the presence of Na^+ and glutamate$^-$ (Fairman *et al*. 1995; Wadiche *et al*. 1995; Arriza *et al*. 1997). Oocytes and other cells have high (around 12 mM) intracellular levels of acidic amino acids (Zerangue and Kavanaugh 1996a). Thus, uptake of radioactive substrates in intact cells reflects a combination of net flux and exchange. Therefore, other systems, such as liposomes inlaid with solubilized transporters, are required for the determination of rates of net flux (Kavanaugh *et al*. 1997).

Recently, a high-resolution crystal structure of a glutamate transporter homologue from the archeon *Pyrococcus horikoshi* was published (Yernool *et al*. 2004). It forms a trimer with a permeation pathway through each of the monomers. The membrane topology of the monomer (Yernool *et al*. 2004) is quite unusual but is in excellent agreement with the topology inferred from biochemical studies (Grunewald *et al*. 1998; Slotboom *et al*. 1999; Grunewald and Kanner 2000). It contains eight transmembrane domains and two oppositely oriented re-entrant loops, one between domains 6 and 7 and the other between domains 7 and 8. The binding pocket is predominantly formed by transmembrane domains 7 and 8 and the two re-entrant loops, which in the

Received February 19, 2006; revised manuscript received May 8, 2006; accepted May 12, 2006.

Address correspondence and reprint requests to Baruch I. Kanner, Department of Biochemistry, Hebrew University Hadassah Medical School, PO Box 12272, Jerusalem 91120, Israel.
E-mail: kannerb@cc.huji.ac.il

Abbreviations used: AA, amino acids; TFB-TBOA, (2*S*,3*S*)-3-{3-[4-(trifluoromethyl)benzoylamino]benzyloxy}-aspartate.

crystal structure enclose a non-protein density presumably corresponding to glutamate (Yernool *et al*. 2004). Importantly, many of the amino acid residues of the transporter inferred to be important in the interaction with sodium (Zhang and Kanner 1999; Borre and Kanner 2001), potassium (Kavanaugh *et al*. 1997; Zhang *et al*. 1998) and glutamate (Bendahan *et al*. 2000) are facing the binding pocket and are close to the non-protein density (Yernool *et al*. 2004). Therefore, we have investigated the possibility of a functional interaction between the driving ions and the substrate. We have exploited the observation that, in the neuronal transporter EAAC-1, not only sodium but also lithium can support uptake of L-aspartate (Borre and Kanner 2001). When lithium replaces sodium, profound and differential changes in the K_m values for the transport currents induced by the different acidic amino acid substrates are observed but not in the K_i of a non-transportable substrate analogue. Thus, the interaction of the substrate with the binding pocket is determined by the nature of the cation at a step after the substrate has bound to the transporter.

Experimental procedures

Transporter constructs

The rabbit glutamate transporter EAAC1 (Kanai and Hediger 1992) with 10 histidines added immediately after the open reading frame followed by the stop codon (Borre and Kanner 2004) in the vector pBluescriptSK(–) (Stratagene, La Jolla, CA, USA) was used to express the transporter in HeLa cells (Keynan *et al*. 1992) in conjunction with the recombinant vaccinia/T7 virus vTF7-3 (Fuerst *et al*. 1986). The histidine-tagged EAAC1 in the vector pOG1 was used for RNA preparation. The latter vector is an oocyte expression vector containing a 5′-untranslated *Xenopus* β-globin sequence and a 3′-poly(A) signal.

cRNA transcription, injection, and oocyte preparation

Capped run-off cRNA transcripts were made from transporter constructs in pOG1 and linearized with *Sac*I using mMessage mMachine (Ambion, Austin, TX, USA), and *Xenopus laevis* oocytes were prepared using collagenase (type 1A, no. C-9891; Sigma, St Louis, MO, USA) and injected as described previously (Borre and Kanner 2001). Oocytes were maintained at 18°C in modified Barth's saline solution [88 mM NaCl, 1 mM KCl, 1 mM $MgSO_4$, 2.4 mM $NaHCO_3$, 1 mM $CaCl_2$, 0.3 mM $Ca(NO_3)_2$, 10 mM HEPES, pH 7.5, with freshly added 2 mM sodium pyruvic acid and 0.5 mM theophylline] supplemented with 10 000 units/L of penicillin, 10 mg/L streptomycin, and 50 mg/L gentamycin.

Oocyte electrophysiology

Oocytes were placed in the recording chamber, penetrated with two agarose-cushioned micropipettes (1%/2 M KCl, resistance varied between 1 and 3 mΩ), voltage clamped using GeneClamp 500 (Axon Instruments, Foster City, CA, USA) and digitized using Digidata 1322 (Axon instruments) both controlled with pClamp9 suite (Axon Instruments). Currents were recorded by using a two-microelectode voltage-clamp circuit (Borre and Kanner 2004). Recording solution contained 96 mM NaCl, 2 mM KCl, 1.8 mM $CaCl_2$, 1 mM $MgCl_2$, 5 mM HEPES–hemisodium, pH 7.5. In cation substitution experiments, NaCl was replaced by equimolar concentrations of LiCl or choline chloride and the HEPES buffer was neutralized with Tris.

Data analysis

Unless stated otherwise, all current–voltage relations represent steady-state net currents $[(I_{buffer + AA}) - (I_{buffer})]$ elicited by the indicated concentrations of the amino acids (AA) L-aspartate, D-aspartate, L-glutamate, L-cysteine or GABA (negative control) and were analysed with Clampfit version 9 (Axon instruments). Data have been normalized to account for variability in expression level within and between different oocyte batches. Data shown are the average from at least three oocytes ± SEM. Where not visible, the SEM was smaller than the size of the symbols. Kinetic parameters were determined by non-linear fitting to the generalized Hill equation using build-in functions of Origin 6.1 (Microcal). In the experiments involving the dependence of the net current on the substrate concentration (L-aspartate, D-aspartate, L-glutamate and L-cysteine), the data points were fitted by lines drawn with parameters determined from fitting net currents (I) with n fixed to 1, and I_{max} (maximum current) and K_m were allowed to vary. For the determination of the dependence of the current on the sodium or lithium concentration, I_{max} was fixed and K_m and n were allowed to vary. The K_i for (2*S*,3*S*)-3-{3-[4-(trifluoromethyl)benzoylamino]-benzyloxy}-aspartate (TFB-TBOA) was determined by analysing the currents induced by L-aspartate in Na^+ as well as in Li^+, in the absence or presence of 1.5 or 2 μM TFB-TBOA.

Reconstitution and transport of radioactive acidic amino acids

Reconstitution of EAAC1 transporters into liposomes was carried out exactly as described for GLT-1 transporters (Kavanaugh *et al*. 1997). The proteoliposomes contained 120 mM KPi, pH 7.4. For net flux measurements, transport reactions were started by adding 10 μL of the EAAC1 proteoliposomes to 360 μL of an external medium containing 150 mM NaCl and 2.5 μM valinomycin (unless stated otherwise), as well as the acidic amino acids at the final concentrations and specific radioactivity indicated in the figure legends. Reactions were terminated at the indicated times as described (Kavanaugh *et al*. 1997). In the case of exchange of accumulated D-[^{3}H]aspartate, 5 μL of the proteoliposomes were actively loaded by diluting them in 45 μL of 150 mM NaCl and 2.5 μM valinomycin and 0.5 μCi of D-[^{3}H]aspartate 37 Ci/mmol. After 12 min, the amount of accumulated D-[^{3}H]aspartate was determined as described (Kavanaugh *et al*. 1997). In other parallel reactions, efflux/exchange was induced after 12 min of influx, by 400-fold dilution of the reaction mixture (50 μL) into 20 mL of the efflux/exchange solutions as indicated in the legend to Fig. 7. These diluted reaction mixtures were filtered either immediately, or after 20 or 60 s. Subsequently, the filters were washed and counted as described (Kavanaugh *et al*. 1997). The filtration of the diluted reaction mixtures took 30 s and therefore the effective times for efflux/exchange, indicated on the abscissa of Fig. 7, were 30, 50 and 90 s. Total protein concentration in the liposomes was determined by the method of Lowry *et al*. (1951). Each experiment was repeated at least three times and triplicate determinations were performed for each time point.

Results

Kinetic parameters of substrate-induced currents

The interaction of acidic amino acid substrates with the transporter in sodium- and lithium-containing media was monitored by measuring the substrate-induced transport currents, because with this method a much wider concentration range can be explored than with uptake of radioactive substrates. In sodium-containing media, saturating concentrations of each of the substrates, L-aspartate, L-glutamate and D-aspartate, induced currents of similar size in oocytes expressing the neuronal transporter EAAC1 (Fig. 1a). The data shown in Fig. 1(a) were recorded at a holding potential of −100 mV, but similar results were obtained at other potentials (data not shown but see Fig. 3). The apparent affinity for the three substrates was also very similar (Fig. 1a and Table 1). When sodium was replaced by lithium, marked differences in the kinetic parameters of the transport currents were observed. The apparent affinity for all three substrates was dramatically reduced (Fig. 1b). Comparing the same oocytes, the maximal induced current by L-aspartate (20 mM) at −100 mV in lithium was 39 ± 8% ($n = 4$) of the current in sodium, induced by 1 mM L-aspartate. Remarkably, even although in lithium medium there was a dramatic increase in the K_m values of the three substrates, this increase was much larger for L-glutamate and D-aspartate. For L-aspartate, the increase in K_m was around 13-fold as compared with an increase of around 130-fold for L-glutamate and D-aspartate (Fig. 1b and Table 1). Even although the apparent affinity for the three substrates in lithium medium was low, the induced currents were specific for the transporter substrates. No currents were induced in lithium-containing medium by 20 mM of GABA, which is not a substrate (Fig. 2). However, L-cysteine, a substrate of low apparent activity (Zerangue and Kavanaugh 1996b), is capable of inducing transport currents in lithium-containing media with an apparent affinity which is around 65-fold lower than that in sodium (Table 1).

The voltage dependence of the currents induced by a saturating concentration of L-aspartate in lithium media was different from that in sodium and resembles earlier results with non-saturating concentrations of L-aspartate (Borre and Kanner 2001). In sodium, the direction of the currents reversed at positive potentials. These outward currents are as a result of the anion-conductance induced by L-aspartate (Wadiche *et al.* 1995). In lithium, no reversal was observed and the currents remained inward at all potentials (Fig. 2). This indicates that, in lithium-containing media, even saturating concentrations of L-aspartate cannot induce the anion conductance. In sodium, the currents reflect the sum of coupled and uncoupled currents. However, there is one holding potential, the reversal potential for chloride, where also in sodium the substrate-induced currents solely represent the coupled current (Wadiche *et al.* 1995). In sodium-containing media at a holding potential of −30 mV, which is near the reversal potential for chloride (Wadiche *et al.* 1995; Zerangue and Kavanaugh 1996a), the apparent affinities for the three substrates were very similar to each other (Fig. 3 and Table 1) and even somewhat higher than those in sodium media at −100 mV (Fig. 1a and Table 1). These observations indicate that the difference in apparent substrate affinities between sodium and lithium media reflects a difference in the electrogenic ion-coupled acidic amino acid translocation.

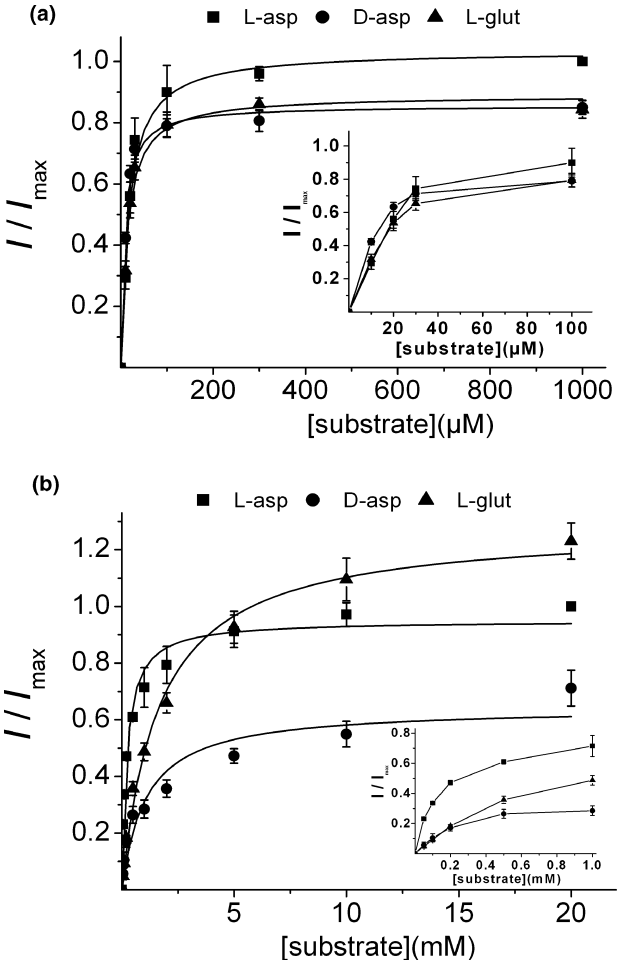

Fig. 1 Concentration dependence of substrate-induced currents mediated by EAAC-1 at −100 mV. The steady-state currents at −100 mV in oocytes expressing EAAC-1 induced by the indicated concentrations of L-aspartate (■), D-aspartate (●) and L-glutamate (▲) in sodium (a) or lithium (b) have been normalized to these induced by 1 mM (a) or 20 mM (b) of L-aspartate. Data are mean ± SE, $n = 3$ or 4 (a, b, respectively). The absolute net currents for 1 mM L-aspartate at −100 mV in sodium Ringer ranged from −465 to −544 nA (a) and for 20 mM L-aspartate at −100 mV in lithium Ringer ranged from −79 to −292 nA (b). Fitting of the data points is described in Experimental procedures. The induced currents at the lower range of substrate concentrations are shown on an expanded scale in the insets.

Table 1 Kinetic constants for substrate-induced currents by EAAC1

	L-aspartate K_m	D-aspartate K_m	D-aspartate I_{maxN}	L-glutamate K_m	L-glutamate I_{maxN}	L-cysteine K_m	L-cysteine I_{maxN}	TFB-TBOA K_i
NaCl (96 mM) −100 mV	17.1 ± 2.9	8.2 ± 1.1	0.86 ± 0.02	13.9 ± 1.8	0.89 ± 0.03	101 ± 5	1.2 ± 0.02	0.62 ± 0.07
NaCl (96 mM) −30 mV	9.8 ± 1.2	3.7 ± 0.5	0.92 ± 0.01	8.0 ± 0.8	0.92 ± 0.02	81.5 ± 5	1.16 ± 0.06	0.59 ± 0.09
NaCl (20 mM) −100 mV	35.9 ± 2.8	31.9 ± 0.8	0.94 ± 0.01	50.6 ± 2.2	0.99 ± 0.01	–	–	–
LiCl (96 mM) −100 mV	223 ± 33	1068 ± 324	0.64 ± 0.05	1644 ± 165	1.28 ± 0.04	6560 ± 729	0.57 ± 0.03	0.88 ± 0.16

The values of K_m (μM) and I_{maxN} were obtained from the currents recorded in sodium and lithium containing recording solutions as described in Experimental procedures. I_{maxN} is defined as the I_{max} value under a given experimental condition relative to the corresponding I_{max} value induced by L-aspartate. The absolute values of these I_{max} values ranged from −465 to −544 nA and from −80 to −135 nA in 96 mM NaCl at −100 and −30 mV, respectively, and from −166 to −321 nA in 20 mM NaCl at −100 mV. The absolute values of I_{max} induced by 20 mM L-aspartate in 96 mM LiCl at −100 mV ranged from −79 to −292 nA. In the case of D-aspartate and L-glutamate in lithium, the fitted currents at this concentration were used to calculate I_{maxN}. The K_i values (μM) were determined using Lineweaver–Burk plots of the values of the currents induced by 10, 20, 30, 50 and 100 μM L-aspartate in the presence and absence of 1.5 μM TFB-TBOA in the sodium-containing medium. In the case of the lithium-containing medium, the L-aspartate concentrations were 100, 200, 300, 500 and 1000 μM with and without 2 μM TFB-TBOA.

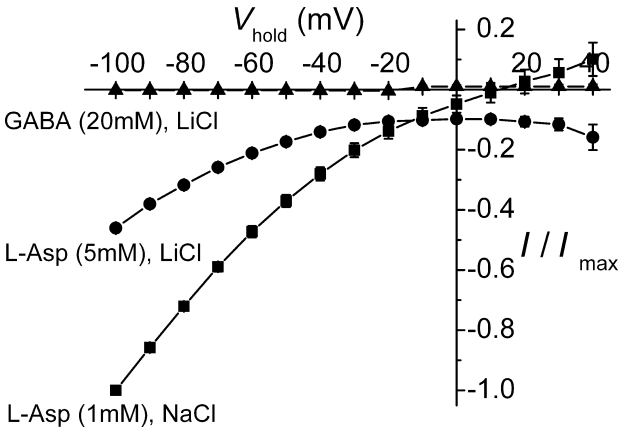

Fig. 2 Cation dependence of L-aspartate-induced currents mediated by EAAC-1. The voltage dependence of steady-state net currents induced by 1 mM L-aspartate in sodium (■), 5 mM L-aspartate in lithium (●) and 20 mM GABA (control) in lithium (▲). All currents are normalized to those induced by 1 mM L-aspartate in sodium Ringer at −100 mV. Data are mean ± SE, $n = 3$ from three different batches of oocytes. The absolute net currents induced by 1 mM L-aspartate in sodium at −100 mV ranged from −465 to −544 nA and those induced by 5 mM L-aspartate in lithium ranged from −214 to −242 nA.

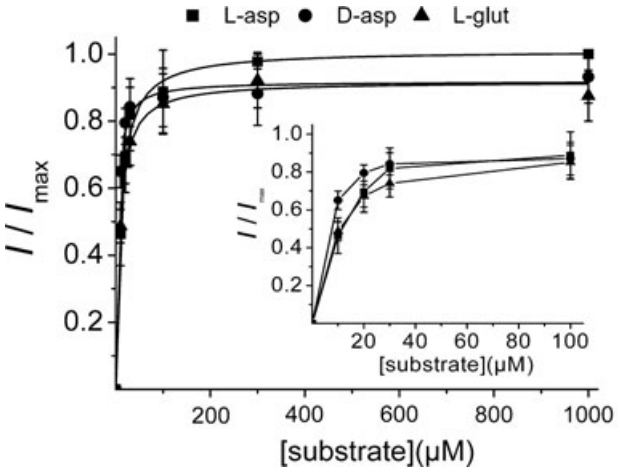

Fig. 3 Concentration dependence of substrate-induced currents mediated by EAAC-1 at −30 mV. The steady-state currents at −30 mV in oocytes expressing EAAC-1 induced by the indicated concentrations of L-aspartate (■), D-aspartate (●) and L-glutamate (▲) in sodium have been normalized to these induced by 1 mM of L-aspartate at −30 mV. Data are mean ± SE, $n = 3$. The absolute net currents for 1 mM L-aspartate at 30 mV in sodium Ringer ranged from −80 to −135 nA. The induced currents at the lower substrate concentrations are shown on an expanded scale in the inset.

It has been proposed that lithium binds to the same sites as sodium, but with a 5–10-fold reduced affinity (Larsson *et al.* 2004). If the differences between the K_m values of the substrates in sodium and lithium would be because of subsaturation of the cation binding sites in lithium, the kinetic parameters in a medium containing only 20 mM sodium (choline substitution) should be similar to those observed in lithium. However, such a reduction of the sodium concentration only led to an increase of the K_m for the three substrates of 2–4-fold (Table 1), which is much smaller than the increase observed in lithium-containing media (Fig. 1 and Table 1). Importantly, the K_m values for the three substrates in 20 mM sodium were also similar to each other (Fig. 4 and Table 1), whereas in lithium there was a marked difference in K_m between L-aspartate on the one

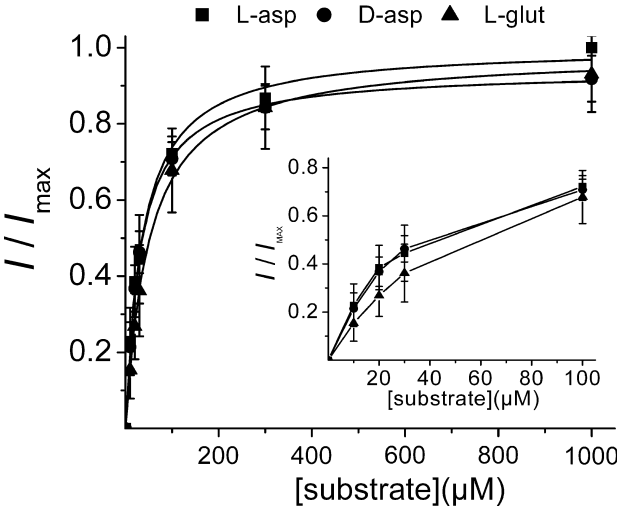

Fig. 4 Concentration dependence of substrate-induced currents mediated by EAAC-1 in media containing 20 mM sodium. The steady-state currents at −100 mV in oocytes expressing EAAC-1 induced by the indicated concentrations of L-aspartate (■), D-aspartate (●) and L-glutamate (▲) in 20 mM sodium (choline substitution) have been normalized to those induced by 1 mM of L-aspartate at −100 mV. Data are mean ± SE, $n = 3$. The absolute net currents for 1 mM L-aspartate at −100 mV in 20 mM sodium ranged from −166 to −321 nA. The induced currents at the lower substrate concentrations are shown on an expanded scale in the inset.

hand and L-glutamate and D-aspartate on the other (Fig. 1b and Table 1).

The marked differences between the K_m values in sodium- and lithium-containing media, may be because of effects of the cations either on substrate binding or on a step in the transport cycle subsequent to binding. In the absence of suitable radioactively labelled binding ligands, we examined this question using the effects of the non-transportable substrate analogue TFB-TBOA (Shimamoto *et al*. 2004), on the currents induced by L-aspartate. TFB-TBOA acted as a competitive blocker in sodium as well as in lithium (Table 1). In contrast to the K_m values for the three substrates, the K_i values were similar in both media (Table 1) and are close to the IC_{50} values of TFB-TBOA on [^{14}C]glutamate uptake by the human counterpart of EAAC1 expressed in cell lines (Shimamoto *et al*. 2004).

Radioactive substrate uptake in reconstituted proteoliposomes

To verify if the difference in apparent substrate affinities between sodium and lithium media is indeed as a result of a difference in the electrogenic ion-coupled acidic amino acid translocation, it is important to use an independent experimental approach; the net influx of the radioactive substrates in the presence of sodium and lithium. However, in intact cells radioactive uptake may reflect either net influx, which requires counter-transport with potassium, and/or exchange with intracellular acidic amino acids (Kavanaugh *et al*. 1997; Zhang *et al*. 1998). Exchange requires the presence of sodium only on one side of the membrane (Kanner and Bendahan 1982; Pines and Kanner 1990) and, therefore, because of the presence of intracellular sodium, could proceed without external sodium (or lithium). To determine the effects of sodium and lithium on net influx, it is necessary to eliminate '*trans*' aspartate and glutamate present in intact cells. Therefore, the EAAC1 transporters were expressed in HeLa cells and, upon subsequent solubilization, they were reconstituted into proteoliposomes containing internal potassium (net influx conditions). Because of the very low apparent affinities observed when substrate-induced currents were measured in oocytes expressing EAAC1 (Table 1), it seemed impossible to measure, in this system, the kinetic parameters of radioactive uptake in the presence of lithium. Nevertheless, in reconstituted liposomes, the K_m for the uptake of acidic amino acids by the glutamate transporter GLT-1 (Pines *et al*. 1992; Zhang and Kanner 1999) is almost one order of magnitude lower than in intact cells expressing this transporter (Arriza *et al*. 1994; Brocke *et al*. 2002), possibly as a result of an effect of an 'unstirred layer' in intact cells. Therefore, we measured transport kinetics of liposomes inlaid with EAAC1 in the presence of external sodium. These liposomes contained internal potassium, which is required for net influx. As transport is electrogenic, the potassium-specific ionophore valinomycin was added, so that a build-up of positive charge on the inside would be offset by the outward movement of potassium ions. Even although, in sodium-containing medium, the uptake is linear with time only for very short periods, we were able to measure initial rates of uptake (20 s). In the EAAC1 proteoliposomes, the K_m values for L-aspartate, L-glutamate and D-aspartate were 0.49 ± 0.10, 1.09 ± 0.21 and 1.01 ± 0.10 μM, respectively ($n = 3$), significantly lower than the K_m values obtained in oocytes (Table 1). The V_{max} values for the three substrates from the same batch of reconstituted proteoliposomes were similar, although there was considerable variation between separate reconstitution experiments. The range for the V_{max} values for the three substrates was from 250 to 1000 pmol/min/mg protein. No L-[^{3}H]aspartate transport was observed upon reconstitution of solubilized proteins from HeLa cells transfected with the empty vector (data not shown). In the presence lithium, significant net flux of L-[^{3}H]aspartate (10 μM) was observed by the liposomes inlaid with the EAAC1 transporter (Fig. 5b), although it appeared slower than that in sodium (Fig. 5a). However, in the presence of choline, no transport could be detected (data not shown). In the presence of either sodium or lithium, the transport was markedly reduced when valinomycin was omitted (Figs 5a and b). Transport was completely inhibited by nigericin (Figs 5a and b). This ionophore is expected to exchange internal potassium for external sodium (or lithium),

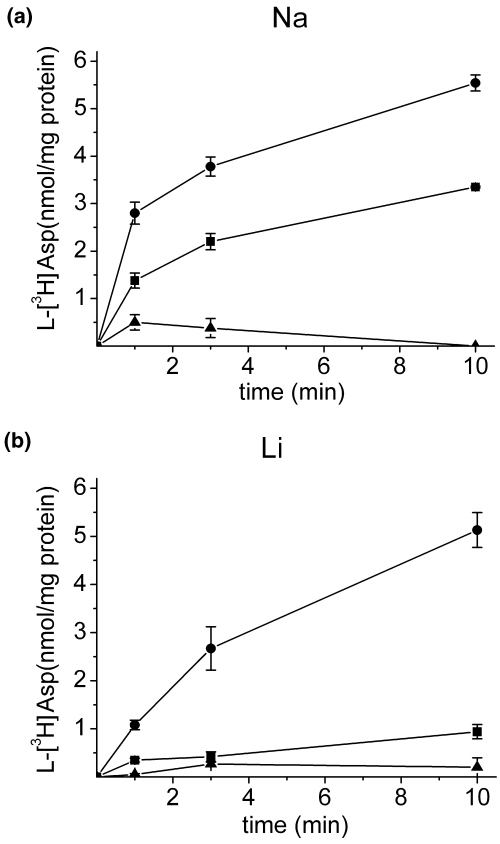

Fig. 5 Effect of ionophores on L-[^{3}H]aspartate uptake by EAAC1 proteoliposomes. EAAC1 was reconstituted in the presence of 0.12 M KPi, as described in Experimental procedures and transport was measured using an external medium containing either 0.15 M NaCl (a) or LiCl (b) and 10 μM L-[^{3}H]aspartate (1.1 Ci/mmol) without ionophore (squares) or with 2.5 μM valinomycin either without (circles) or with 5 μM nigericin (triangles). Reactions were terminated at the indicated times and each time point was performed in triplicate.

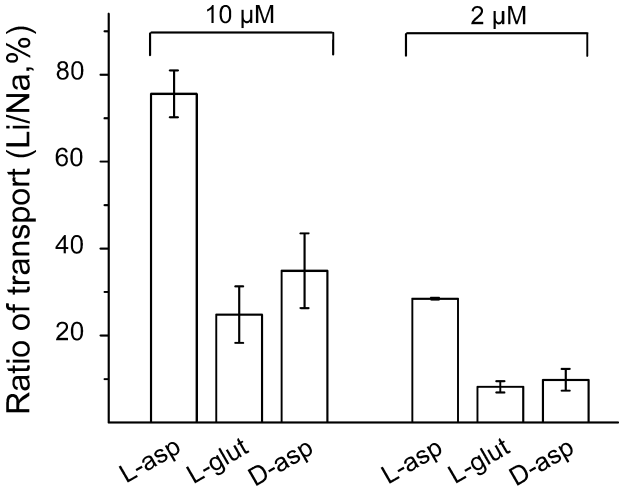

Fig. 6 Ratio of [^{3}H]acidic amino acid transport in lithium- and sodium-containing media. Transport of L-[^{3}H]aspartate, L-[^{3}H]glutamate, and D-[^{3}H]aspartate was measured for 10 min both in 0.15 M NaCl and in 0.15 M LiCl, using a final concentration of 10 or 2 μM, and the amount of radioactive label added was 4 or 2 μCi, respectively. The specific radioactivity of L-[^{3}H]aspartate, L-[^{3}H]glutamate and D-[^{3}H]aspartate was 37, 49 and 37 Ci/mmol, respectively.

and thereby to collapse the artificially imposed ion gradients, which are the driving forces for transport.

As opposed to the situation in sodium, the initial rates of net flux of radioactively labelled substrates in lithium were too low to permit reliable determination of the kinetic parameters. In order to address the question, if in the reconstituted system L-aspartate is also the preferred substrate in the presence of lithium, we tested the net uptake of radioactive L-aspartate, L-glutamate and D-aspartate in sodium- and lithium-containing media at longer times, where transport is not linear anymore. Under such conditions, we found that the ratio of the net flux values in lithium to those in sodium was considerably higher for L-aspartate than for L-glutamate or D-aspartate (Fig. 6). This was true at both concentrations where the substrates were tested: 2 and 10 μM (Fig. 6).

A possible explanation for the lower apparent substrate affinity in lithium could be that the second step in the catalytic cycle, the translocation of potassium, is affected by lithium. In order to address this possibility, the effect of lithium on the exchange reaction, which is potassium-independent, was determined. D-[^{3}H]Aspartate was first loaded into the EAAC1 proteoliposomes by active transport and subsequently the reaction mixtures were diluted 400-fold into sodium- or lithium-containing solutions without (net efflux) or with L-glutamate (exchange). The accumulated D-[^{3}H]aspartate did not leave the proteoliposomes, even after a 400-fold dilution into a solution containing sodium (Fig. 7a) or lithium (Fig. 7b). However, when these solutions were supplemented with 1 mM L-glutamate, a condition enabling exchange of labelled internal with unlabelled external substrates (Kanner and Bendahan 1982; Kavanaugh *et al*. 1997), a rapid exit of the D-[^{3}H]aspartate took place (Figs 7a and b). No such exit took place when the external solution contained choline, with or without 1 mM L-glutamate (data not shown). At 6 μM L-glutamate, around 5–6-fold the K_m for L-glutamate in the proteoliposomes in sodium, the exchange in the presence of sodium was almost as rapid as with 1 mM L-glutamate (Fig. 7a). However, in the presence of lithium, almost no exchange was detectable in the presence of 6 μM L-glutamate (Fig. 7b), presumably because of the reduced apparent affinity of the transporter for glutamate in the presence of this cation.

Discussion

Until recently, it was believed that only extracellular sodium ions could support amino acid transport through eukaryotic glutamate transporters, even although lithium was found to

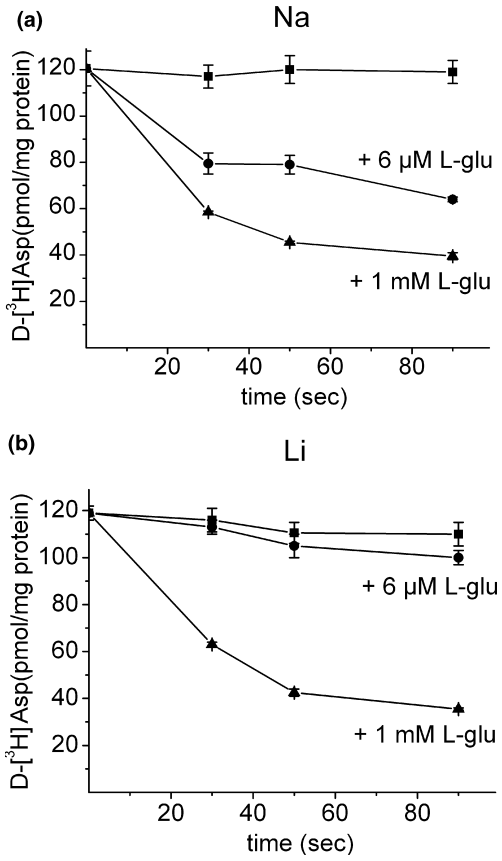

Fig. 7 Efflux and exchange of D-[^{3}H]aspartate after prior active loading into EAAC1 proteoliposomes. EAAC1 proteoliposomes were 'actively' loaded and efflux/exchange was initiated as described in Experimental procedures. The efflux/exchange solutions contained 0.15 M NaCl (a) or LiCl (b) without (■) or with 6 μM (●) or 1 mM (▲) L-glutamate. Reactions were terminated at the indicated times and each time point was performed in triplicate.

replace at least one sodium ion in GLT-1 (Grunewald and Kanner 1995). Recently, we found that, in the neuronal glutamate transporter EAAC1, L-aspartate induces inwardly rectifying steady-state currents in the presence of Li^+ (Borre and Kanner 2001), suggesting that in this transporter Li^+ can replace Na^+ at all Na^+-binding sites. Subsequent observations suggested that Li^+ binds to the same cation-binding sites and induces the same conformational changes as does Na^+, but with a 5-to 10-fold lower affinity (Larsson *et al*. 2004). In the present study, we found that replacement of Na^+ by Li^+ dramatically changes the kinetic parameters of acidic amino acid transport. A possible explanation could be a change in stoichiometry when lithium replaces sodium. However, the substrate discrimination by the transporter is also altered, such that L-aspartate becomes the preferred substrate (Fig. 1 and Table 1). The K_m for L-aspartate is increased around 13-fold, whereas for the other two substrates the increase is much larger, around 130-fold (Fig. 1 and Table 1). This changed substrate discrimination is not easy to explain by an altered stoichiometry. When the neutral cysteine replaces the negatively charged acidic amino acids as a substrate, the charge translocated by the human homologue of EAAC1 apparently does not change, because the internal acidification observed during acidic amino acid transport is not seen with cysteine (Zerangue and Kavanaugh 1996a). Thus, the stoichiometry for sodium appears to be a fixed parameter and probably is not changed in the presence of lithium, even although this possibility cannot be strictly excluded. In the presence of Li^+, the change of the I_{max} for L-aspartate is much smaller than that of K_m, only around 2.5-fold. Nevertheless, the decrease suggests that it is not just substrate binding that is changed when the cation is replaced. Actually, inhibition studies, with the competitive non-transportable substrate analogue TFB-TBOA, show that there is only a minimal change in K_i when Na^+ is replaced by Li^+ (Table 1). Thus, the effect of the coupling ion on the specificity of the substrates is introduced in a step after their binding to the transporter. These observations are in agreement with earlier studies on GLT-1, which showed that replacement of sodium by lithium had a marked impact on the kinetic parameters of transportable substrates, but only a minor effect on the K_i for the non-transportable analogue dihydrokainate (Zhang and Kanner 1999). The expression of EAAC1 in oocytes is much more robust than that of GLT-1 and this enabled us to measure the substrate-induced transport currents in sodium as well as in lithium over a wide concentration range and to make the novel observation that L-aspartate is the preferred EAAC1 substrate in the presence of lithium.

In the recent models of the glutamate transport cycle, two sodium ions bind before the acidic amino acid substrate, and subsequent substrate binding enables the binding of the third cation (Watzke *et al*. 2001; Bergles *et al*. 2002). Whereas lithium and sodium are equivalent in the binding to the first two sites, this is not the case for the third cation which interacts with the substrate-bound transporter. This difference could be at the binding step itself, but could also be at a later step such as the translocation or the de-binding of one of the cations on the intracellular side, but apparently not at the potassium translocation step. If the latter were the case, there should be no effect of replacing sodium with lithium in the exchange reaction, but this was not observed (Fig. 7).

Because of the dramatic reduction in the apparent affinity of the substrates tested, we were initially doubtful if we could show that L-aspartate is the preferred substrate in lithium using direct net flux of radioactive substrates. In contrast to the transport currents, the determination of the kinetic parameters using radioactive measurements is dependent not only on V_{max} but also by the apparent affinity because of limitations in the specific radioactivity which can be applied. Nevertheless, we could demonstrate that the ratio of uptake

in lithium versus that in sodium is significantly higher for L-[^{3}H]aspartate than for L-[^{3}H]glutamate or D-[^{3}H]aspartate (Fig. 6). Importantly, radioactive uptake of L-aspartate in lithium exhibited all the hallmarks of electrogenic net flux, just like that observed in sodium (Fig. 5). An interesting difference is that the degree of stimulation of transport by valinomycin (i.e. the ability to prevent build-up of positive charge because of electrogenic transport) is larger in lithium than in sodium (Fig. 5). A possible explanation is that the apparent affinity of the transporter for lithium is smaller than that for sodium (Larsson *et al*. 2004). Thus, it is likely that, in the absence of an artificially applied interior negative membrane potential, less transporters are binding lithium than sodium. Alternatively, it is possible that the anion leak pathway, which is open in the presence of sodium but not of lithium (Borre and Kanner 2001), allows some charge compensation.

How could the nature of the co-transported cation influence the conformation of the binding pocket? The ionic diameter of Li^+ is smaller than that of Na^+. It is possible that, because of its larger size, an additional group participates in the liganding of Na^+. An example for this idea is illustrated by the structural analysis of dialkylglycine decarboxylase (Toney *et al*. 1993). Dialkylglycine decarboxylase specifically requires K^+ for activity. However, in the absence of K^+, the smaller Na^+ can fit tightly in the binding site with coordination to five oxygen ligands. With the larger K^+ bound, the cation binding cavity enlarges by 0.8Á, and the number of coordination oxygens increases from five to six by enclosing an additional hydroxyl group to the cation coordination sphere. As for the neuronal transporter EAAC-1, it is possible that, for the smaller Li^+ ion, less liganding groups are required than for Na^+. The extra group involved in the coordination of sodium could come from a main-chain or side-chain atom of the binding pocket. The contribution of such a liganding group could bring about a change in the way the substrate is bound to the transporter. In principle, the extra liganding group could also be provided by the co-transported substrate; in other words, in one of the conformations the transporter is going through during the translocation process, one of the groups on the substrate could even make direct contact with one of the sodium ions. In this case, this is unlikely to be the γ-carboxyl group of glutamate or the β-carboxyl group of aspartate, as the pronounced difference in apparent affinity is also observed with the transport currents induced by cysteine, which does not have an 'extra' carboxyl group (Table 1). Remarkably, while this paper was in preparation, a direct example of a physical contact between the 'driving' ion and the 'driven' substrate was published. The carboxyl group of leucine was found to make direct contact with one of the two sodium ions of the leucine transporter $LeuT_{Aa}$, a bacterial homologue of the Na^+/CL^--dependent neurotransmitter transporters (Yamashita *et al*. 2005). One possibility would be that, in the glutamate transporters, the α-carboxyl group could be a liganding group for sodium.

In the crystal structure of the glutamate transporter homologue (Yernool *et al*. 2004), the resolution is not sufficiently high to observe cations in the binding pocket. However, a non-protein density, likely representing glutamate, is observed. Many of the amino acid residues equivalent to those inferred to be important for the interaction of the eukaryotic transporters with sodium (Zhang and Kanner 1999; Borre and Kanner 2001), potassium (Kavanaugh *et al*. 1997; Zhang *et al*. 1998) and glutamate (Bendahan *et al*. 2000) are facing the binding pocket and are close to the non-protein density (Yernool *et al*. 2004). These observations, as well as the functional data presented here, are consistent with the idea of a direct contact of one or more of the sodium ions with glutamate. However, it is nevertheless possible that the effect of the cation on substrate specificity is as a result of conformational changes over a relatively short distance in the binding pocket. To resolve this issue, a higher-resolution structure of a glutamate transporter, perhaps of a different conformation is needed.

Acknowledgements

This work was supported by grant NS 16708 from the NINDS, NIH and the Bernard Katz Minerva Center for Cellular Biophysics**.** We thank Dr Keiko Shimamoto for providing us with TFB-TBOA and Elia Zomot for his help in the preparation of the Figures.

References

Arriza J. L., Fairman W. A., Wadiche J. I., Murdoch G. H., Kavanaugh M. P. and Amara S. G. (1994) Functional comparisons of three glutamate transporter subtypes cloned from human motor cortex. *J. Neurosci.* **14**, 5559–5569.

Arriza J. L., Eliasof S., Kavanaugh M. P. and Amara S. G. (1997) Excitatory amino acid transporter 5, a retinal glutamate transporter coupled to a chloride conductance. *Proc. Natl Acad. Sci. USA* **94**, 4155–4160.

Bendahan A., Armon A., Madani N., Kavanaugh M. P. and Kanner B. I. (2000) Arginine 447 plays a pivotal role in substrate interactions in a neuronal glutamate transporter. *J. Biol. Chem.* **275**, 37 436–37 442.

Bergles D. E., Tzingounis A. V. and Jahr C. E. (2002) Comparison of coupled and uncoupled currents during glutamate uptake by GLT-1 transporters. *J. Neurosci.* **22**, 10 153–10 162.

Borre L. and Kanner B. I. (2001) Coupled, but not uncoupled, fluxes in a neuronal glutamate transporter can be activated by lithium ions. *J. Biol. Chem.* **276**, 40 396–40 401.

Borre L. and Kanner B. I. (2004) Arginine 445 controls the coupling between glutamate and cations in the neuronal transporter EAAC-1. *J. Biol. Chem.* **279**, 2513–2519.

Brew H. and Attwell D. (1987) Electrogenic glutamate uptake is a major current carrier in the membrane of axolotl retinal glial cells. *Nature* **327**, 707–709.

Brocke L., Bendahan A., Grunewald M. and Kanner B. I. (2002) Proximity of two oppositely oriented re-entrant loops in the glutamate transporter GLT-1 identified by paired cysteine mutagenesis. *J. Biol. Chem.* **277**, 3985–3992.

Fairman W. A., Vandenberg R. J., Arriza J. L., Kavanaugh M. P. and Amara S. G. (1995) An excitatory amino-acid transporter with properties of a ligand-gated chloride channel. *Nature* **375**, 599–603.

Fuerst T. R., Niles E. G., Studier F. W. and Moss B. (1986) Eukaryotic transient-expression system based on recombinant vaccinia virus that synthesizes bacteriophage T7 RNA polymerase. *Proc. Natl Acad. Sci. USA* **83**, 8122–8126.

Grunewald M. and Kanner B. (1995) Conformational changes monitored on the glutamate transporter GLT-1 indicate the existence of two neurotransmitter-bound states. *J. Biol. Chem.* **270**, 17 017–17 024.

Grunewald M. and Kanner B. I. (2000) The accessibility of a novel re-entrant loop of the glutamate transporter GLT-1 is restricted by its substrate. *J. Biol. Chem.* **275**, 9684–9689.

Grunewald M., Bendahan A. and Kanner B. I. (1998) Biotinylation of single cysteine mutants of the glutamate transporter GLT-1 from rat brain reveals its unusual topology. *Neuron* **21**, 623–632.

Kanai Y. and Hediger M. A. (1992) Primary structure and functional characterization of a high-affinity glutamate transporter. *Nature* **360**, 467–471.

Kanner B. I. and Bendahan A. (1982) Binding order of substrates to the sodium and potassium ion coupled L-glutamic acid transporter from rat brain. *Biochemistry* **21**, 6327–6330.

Kanner B. I. and Sharon I. (1978) Active transport of L-glutamate by membrane vesicles isolated from rat brain. *Biochemistry* **17**, 3949–3953.

Kavanaugh M. P., Bendahan A., Zerangue N., Zhang Y. and Kanner B. I. (1997) Mutation of an amino acid residue influencing potassium coupling in the glutamate transporter GLT-1 induces obligate exchange. *J. Biol. Chem.* **272**, 1703–1708.

Keynan S., Suh Y. J., Kanner B. I. and Rudnick G. (1992) Expression of a cloned γ-aminobutyric acid transporter in mammalian cells. *Biochemistry* **31**, 1974–1979.

Larsson H. P., Tzingounis A. V., Koch H. P. and Kavanaugh M. P. (2004) Fluorometric measurements of conformational changes in glutamate transporters. *Proc. Natl Acad. Sci. USA* **101**, 3951–3956.

Levy L. M., Warr O. and Attwell D. (1998) Stoichiometry of the glial glutamate transporter GLT-1 expressed inducibly in a Chinese hamster ovary cell line selected for low endogenous Na^+-dependent glutamate uptake. *J. Neurosci.* **18**, 9620–9628.

Lowry O. H., Rosebrough N. J., Farr A. L. and Randall R. J. (1951) Protein measurement with the Folin phenol reagent. *J. Biol. Chem.* **193**, 265–275.

Pines G. and Kanner B. I. (1990) Counterflow of L-glutamate in plasma membrane vesicles and reconstituted preparations from rat brain. *Biochemistry* **29**, 11 209–11 214.

Pines G., Danbolt N. C., Bjoras M., Zhang Y., Bendahan A., Eide L., Koepsell H., Storm-Mathisen J., Seeberg E. and Kanner B. I. (1992) Cloning and expression of a rat brain L-glutamate transporter. *Nature* **360**, 464–467.

Shimamoto K., Sakai R., Takaoka K., Yumoto N., Nakajima T., Amara S. G. and Shigeri Y. (2004) Characterization of novel L-threo-β-benzyloxyaspartate derivatives, potent blockers of the glutamate transporters. *Mol. Pharmacol.* **65**, 1008–1015.

Slotboom D. J., Sobczak I., Konings W. N. and Lolkema J. S. (1999) A conserved serine-rich stretch in the glutamate transporter family forms a substrate-sensitive re-entrant loop. *Proc. Natl Acad. Sci. USA* **96**, 14 282–14 287.

Toney M. D., Hohenester E., Cowan S. W. and Jansonius J. N. (1993) Dialkylglycine decarboxylase structure: bifunctional active site and alkali metal sites. *Science* **261**, 756–759.

Wadiche J. I., Amara S. G. and Kavanaugh M. P. (1995) Ion fluxes associated with excitatory amino acid transport. *Neuron* **15**, 721–728.

Watzke N., Bamberg E. and Grewer C. (2001) Early intermediates in the transport cycle of the neuronal excitatory amino acid carrier EAAC1. *J. Gen. Physiol.* **117**, 547–562.

Yamashita A., Singh S. K., Kawate T., Jin Y. and Gouaux E. (2005) Crystal structure of a bacterial homologue of Na^+/Cl-dependent neurotransmitter transporters. *Nature* **437**, 215–223.

Yernool D., Boudker O., Jin Y. and Gouaux E. (2004) Structure of a glutamate transporter homologue from *Pyrococcus horikoshii*. *Nature* **431**, 811–818.

Zerangue N. and Kavanaugh M. P. (1996a) Flux coupling in a neuronal glutamate transporter. *Nature* **383**, 634–637.

Zerangue N. and Kavanaugh M. P. (1996b) Interaction of L-cysteine with a human excitatory amino acid transporter. *J. Physiol.* **493**, 419–423.

Zhang Y. and Kanner B. I. (1999) Two serine residues of the glutamate transporter GLT-1 are crucial for coupling the fluxes of sodium and the neurotransmitter. *Proc. Natl Acad. Sci. USA* **96**, 1710–1715.

Zhang Y., Bendahan A., Zarbiv R., Kavanaugh M. P. and Kanner B. I. (1998) Molecular determinant of ion selectivity of a (Na^+ + K^+)-coupled rat brain glutamate transporter. *Proc. Natl Acad. Sci. USA* **95**, 751–755.